Journal of Geointerface, Vol. 5, No. 1, July 2026, pp. 96–114 e-ISSN: 2583-6900

Contrasting petrogenesis of charnockites across the Kasargod–Mercara Shear Zone, southern India

Saumyaranjan Nanda, S Rekha*

Department of Earth and Atmospheric Sciences, National Institute of Technology Rourkela Odisha 769008, India

ABSTRACT

This study presents an integrated petrographic and geochemical investigation of charnockites from the southern part of the Western Dharwar Craton (WDC), Coorg Block (CB), and the Kasargod–Mercara Shear Zone (KMSZ) separating the two crustal domains, with the aim of constraining their petrogenesis and tectonic setting. The charnockites from the three different domains display diverse textural and compositional characteristics reflecting their contrasting tectonomagmatic histories. Petrographically, WDC charnockites are foliated, medium-grained, and exhibit hornblende-biotite retrogression, while CB charnockites are coarse-grained and massive with limited retrograde alteration. KMSZ charnockites are strongly deformed, showing dynamic recrystallization textures. Geochemically, WDC charnockites are metaluminous, ferroan, and high-K with tholeiitic affinity, suggesting derivation from an evolved, crustally contaminated melt in a post-collisional setting. In contrast, CB charnockites are low-K, calcic, and magnesian with metaluminous compositions, suggestive of mantle-derived magmas generated in a subduction-related arc environment. The KMSZ charnockites are peraluminous to metaluminous, calc-alkaline, and magnesian, pointing to a mixed crustal-mantle source influenced by shear zone-related deformation and crustal assimilation in a convergent margin or syn-collisional regime. These findings reveal complex magma generation processes and tectonic evolution along the accretion window between the WDC and CB.

ARTICLE HISTORY

Received: 19 March 2026
Revised: 30 April 2026
Accepted: 01 May 2026

https://doi.org/10.5281/zenodo.20043058

KEYWORDS

Western Dharwar Craton
Coorg Block
Kasargod–Mercara Shear Zone
Southern Granulite Terrane
Charnockite

1. Introduction

The southern Indian shield, particularly the Western Dharwar Craton (WDC) and its adjoining high-grade granulite terrane i.e. Southern Granulite Terrane (SGT), preserves a complex record of crustal growth, reworking, and tectonothermal events spanning from Neoarchean to Paleoproterozoic (Jayananda et al., 2013a,b; Peucat et al., 2013; Santosh et al., 2015). The southern part of the relatively stable WDC is separated from the deeply reworked Coorg Block (CB) – the northwestern crustal block of the SGT – by the Kasargod–Mercara Shear zone (KMSZ) (Sunil et al., 2010; Chetty et al., 2012; Amaldev et al., 2016; Rekha et al., 2014) (Fig. 1). These terranes, including the WDC, CB and the intervening KMSZ, represent key segments of the continental crust that have undergone extensive magmatic, metamorphic, and deformational processes (Jayananda et al., 2013a,b; Santosh et al., 2015). The CB represents a high-grade fragment of the SGT, with structural and metamorphic imprints reflecting deep crustal reworking during late Neoarchean tectonothermal events (Basak et al., 2023; Santosh et al., 2015; Yang et al., 2023). The KMSZ is characterized by pervasive shearing, high-grade metamorphism, and localized zones of incipient charnockitization, where amphibolite-facies gneisses are transformed into charnockitic rocks through fluid-assisted reactions (Santosh et al., 2004).

*Corresponding author. Email: georekha@gmail.com (SR), srnanda.sonu@gmail.com (SN)

A characteristic lithology of these high-grade domains is the presence of charnockite—orthopyroxene-bearing granitoids formed under granulite-facies conditions, often linked to deep crustal anatexis, fluid-deficient metamorphism, or CO_2-rich metasomatism (Harley, 1989). Charnockitic rocks occur across all three domains—WDC, KMSZ, and the CB—showing considerable variability in texture, mineralogy, and chemical composition. These rocks preserve critical geochemical and petrological signatures that can shed light on lower crustal processes, including melt generation, fractional crystallization, and crust-mantle interactions (Peucat et al., 1993; Jayananda et al., 2015). Geochemical characterization, especially using major element systematics, offers initial constraints on the petrogenesis, source composition, and tectonic setting of charnockitic rocks (Frost et al., 2001; Moyen, 2009).

The WDC granitoid and charnockite emplacement occurred between 2.6 and 2.55 Ga (Jayananda et al., 2013a,b; Peucat et al., 1995), following earlier CB arc magmatism and metamorphism dated between 3.1 and 2.9 Ga (Santosh et al., 2015). Later, the KMSZ experienced transpression and crustal reworking around 2.4 Ga (Rekha et al., 2014; Amaldev et al., 2016). These ages represent multiple crust-forming episodes, collectively support the inference that the compositional diversity across the zone reflects progressive crustal accretion and reworking from the Meso- to Neoarchean.

While prior studies (e.g., Santosh et al., 2014; Amaldev et al., 2016) have established metamorphic, geochemical, and isotopic characteristics from these domains independently, the geochemical characterization across all three domains have not been systematically compared using fresh, uniformly analyzed datasets. This paper quantifies the major oxide variations (SiO_2, FeO, MgO, CaO, K_2O, Na_2O, TiO_2) to evaluate magma differentiation, fluid interaction, and crustal input across domains, thereby testing petrogenetic models inferred from prior isotopic work. It further examines the tectonic interface role of the KMSZ as an "accretionary window," a key zone where compositional variations may record the transition from subduction-related to collision-related magmatism. This study uses an integrated petrographic-geochemical approach to understand the evolution of the charnockites across this terrane.

The present study focuses on the geochemical characterization of charnockites from three spatially and tectonically distinct domains: (1) the Western Dharwar Craton, (2) the Kasargod–Mercara Shear Zone, and (3) the Coorg Block. By analyzing major element compositions, we aim to assess the petrogenetic pathways of charnockite formation, evaluate the tectonic regimes under which these rocks evolved and provide insights into the crustal architecture and evolution of the southern Indian shield during the late Archean and early Proterozoic. The results obtained in this study compared with the existing data for a better understanding of the tectonic evolution of both the crustal blocks.

2. Regional geology

2.1. Western Dharwar Craton

The Dharwar craton is one of the best-studied terrains of Peninsular India, and is renowned for its greenstone/schist belts, grey gneisses, charnockites and younger granites. The craton is divided into two tectonic blocks after Swami Nath et al. (1976), viz., the Western Block and the Eastern Block, renamed respectively as the Western Dharwar Craton (WDC) and Eastern Dharwar Craton (EDC) by Rogers (1986). The shear zone delineating the eastern boundary of the Chitradurga greenstone belt is recognised as the interface between the WDC and EDC (Chardon et al., 2008) (Fig. 1). However, in the southern and northernmost parts of the craton, this boundary is not clearly defined. The migmatitic tonalitic gneisses that make up the WDC are older than 3.0 Ga and are referred to as Peninsular gneisses (Beckinsale et al., 1980; Taylor et al., 1984; Dhoundial et al., 1987; Peucat et al., 1989, 1993; Friend and Nutman, 1991; Meen et al., 1992; Nutman et al., 1996; Chardon et al., 2011; Sarma et al., 2011). Two distinct categories of greenstone belts are recognized within the WDC (Ramakrishnan et al., 1976; Swami Nath et al., 1976; Swami Nath and Ramakrishnan, 1981). The Sargur Group, dated around 3.3 Ga (Peucat et al., 1995; Jayananda et al., 2008) and the Dharwar Supergroup that encompasses Bababudan–Western Ghats–Shimoga belt dated 3.0–2.9 Ga (Peucat et al., 1995; Trendall et al., 1997; Rekha et al., 2013) along with the Chitradurga–Gadag belt dated 2.6–2.55 Ga (Jayananda et al., 2013a,b).

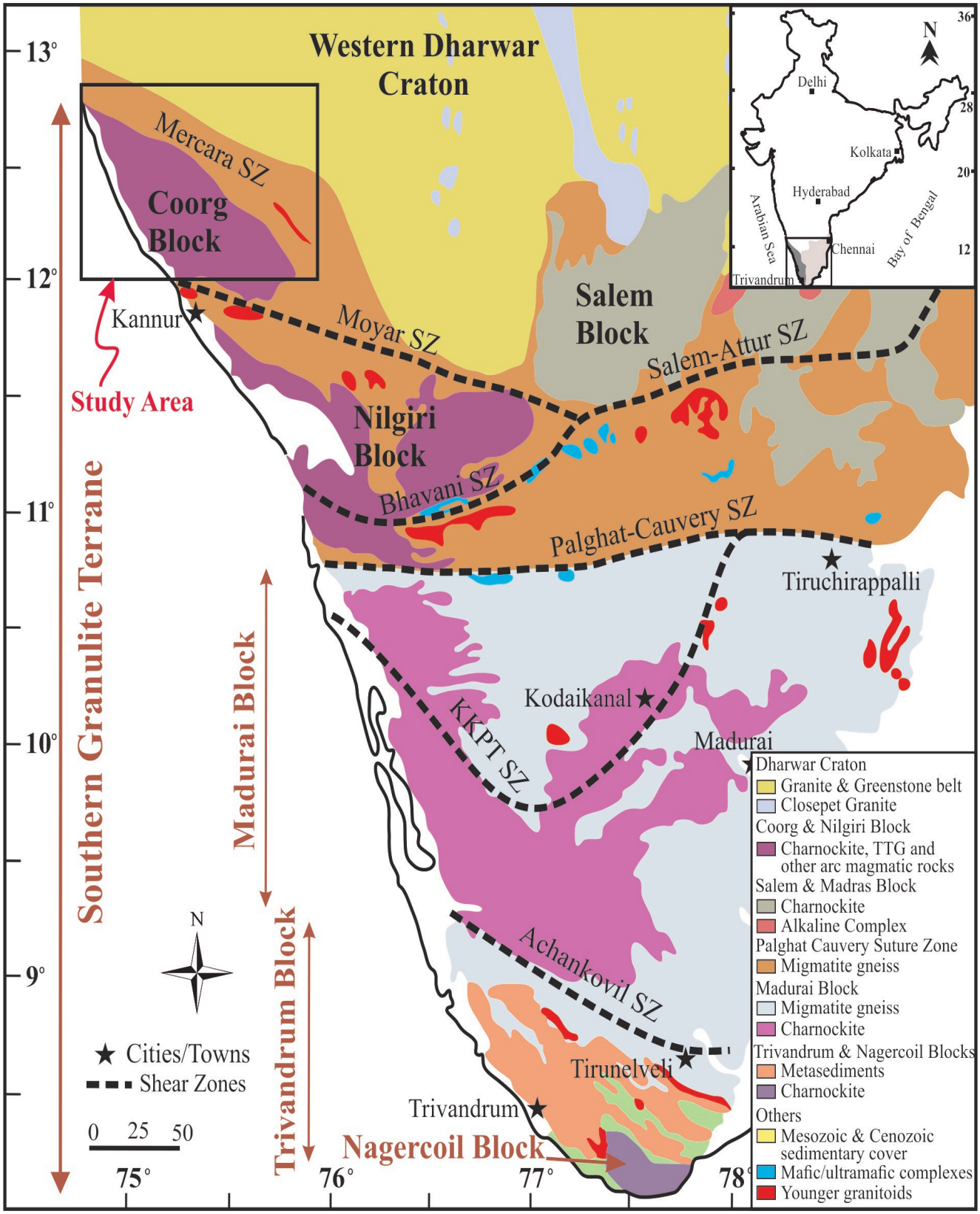

Fig. 1. Generalized geological map of the study area (after Praharaj and Rekha, 2022) shows the Southern Granulite Terrane with distinct crustal domains and the shear zones separating them. Black box shows the study area. SZ – Shear Zone; KKPT – Karur–Kambam–Painavu–Trichur. Inset map shows the enlarged region along the southern part of India.

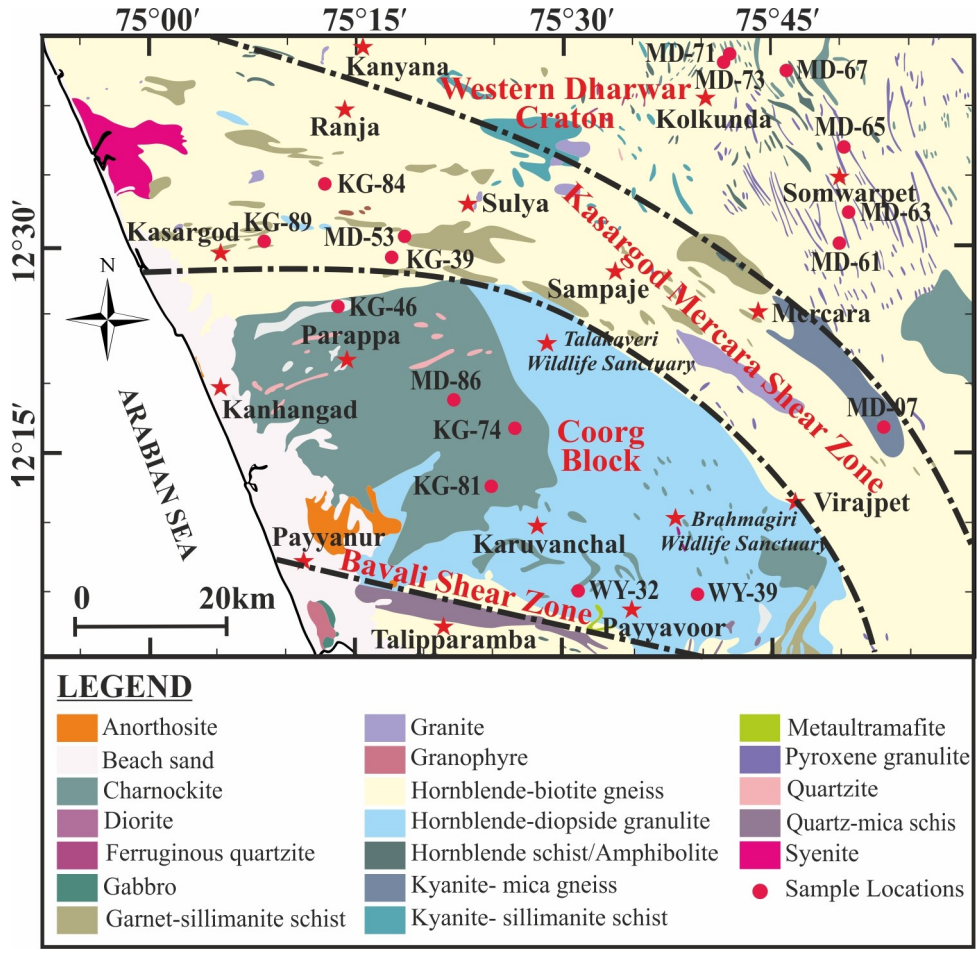

Fig. 2. Enlarged view of the study area marked in Fig. 1. Locations of samples selected for the geochemical analyses shown by filled circles (red colour). Filled stars (red colour) are the important key localities within study area.

Although the WDC is largely characterized by greenschist to amphibolite-facies metamorphism, localized occurrences of charnockitic rocks have been reported (Raith et al., 1989; Naha et al., 1993; Bhattacharya and Sen, 2000; Bhattacharya and Chaudhary, 2013) (Fig. 2). Based on structural data, Naha et al. (1993) concluded that the charnockites of the Dharwar craton have evolved in at least two distinct phases that are separated both in time and in process. The charnockites in the WDC occur both as patchy intrusions and as transformation zones within gneissic host rocks. These occurrences are frequently spatially associated with ductile shear zones (e.g., near Kabbaldurga), fold noses, and other structural discontinuities, suggesting that structural controls played a key role in channelizing metamorphic fluids (Stähle et al., 1987). Fluid inclusion studies and field relationships indicate that the transformation from amphibolite- to granulite-facies assemblages was triggered by CO_2-rich fluids, likely derived from deeper granulitic crust (Raith et al., 1989; Santosh et al., 2004). Additionally, the presence of mafic granulite enclaves in the same area indicates an earlier granulite-facies event, predating the patchy charnockitization observed in the region (Bhattacharya and Sen, 2000). However, Kabbaldurga favors an in situ transformation mechanism driven by CO_2-fluid ingress (Ravindra Kumar and Venkatesh Raghavan, 1992, Srikantappa et al., 1992, Santosh and Tsunogae, 2003).

2.2. Coorg Block

The CB located at the northwestern margin of the SGT (Fig. 1) is considered as one of the oldest crustal blocks in the SGT (Santosh et al., 2015, 2016). The CB is a granulite-facies terrane composed predominantly of charnockites, pyroxene granulites, and migmatitic gneisses that are found in large-scale massifs (Asha Manjari and Malur, 1997) (Figs. 1, 2). Interspersed mafic granulite enclaves represent relict lower crustal fragments. CB also hosts anorthosites,

gabbros, and diorites, likely of mantle origin (Santosh et al., 2015). Local metasedimentary units and sheared gneisses present along the bounding shear zones suggest episodes of supracrustal accretion and tectonic reworking.

CB charnockites are tonalitic to granitic in composition and were formed under high-temperature, CO_2-rich conditions, indicative of deep crustal metamorphism (Santosh et al., 2004). Previous studies suggest CB charnockites are related to arc magmatic processes, comprising a suite of felsic volcanic tuffs and granitoid associated with tonalite-trondhjemite-granodiorite (TTG) gneisses (Santosh et al., 2004; Yang et al., 2023). The study proposes contemporaneous mafic and felsic magmatism, marked by magma mingling and mixing, indicative of an arc tectonic setting. This interpretation is further supported by major, trace, and rare earth element (REE) geochemistry, which reveals subduction-related signatures in the representative rock types of the CB, implying magma generation in a convergent margin environment (Santosh et al., 2014; Yang et al., 2023). The CB charnockites are probably the vestiges of Mesoarchean arc magmatism and crust building. Available geochronological data suggest a maximum age of 3.1 Ga for the CB with a granulite facies metamorphism at around 2.9 Ga, which followed the magmatic emplacement (Santosh et al., 2015; Yang et al., 2023).

2.3. Kasargod–Mercara Shear Zone

The Kasargod–Mercara Shear Zone (KMSZ) is a curvilinear transpressional shear zone sandwiched between the WDC on its north and CB on its south (Sunil et al., 2010; Chetty et al., 2012; Rekha et al., 2014; Anoop et al., 2022; Yu et al., 2022) (Figs. 1, 2). KMSZ wraps around the CB along its northern border and is over 20–30 km wide and 100 km long dextral shear zone (Chetty et al., 2012; Rekha et al., 2014). Charnockites, TTG gneisses, metagabbros, mafic granulites, kyanite-sillimanite bearing metapelites (khondalites), staurolite-kyanite-garnet-sillimanite bearing pelites, banded magnetite quartzites, pyroxene granulites, and quartz mica schists are some of the main rock types found in the shear zone. There are also younger granitic and syenitic intrusives (Santosh et al., 2014, Amaldev et al., 2016). The structural studies by Rekha et al. (2014) described the KMSZ as a sub vertical dextral transpressional shear zone of 2.3–2.4 Ga age. Whereas igneous zircons in the magmatic suite suggest prominent convergent margin magmatism during 3.1 to 3.2 Ga (Amaldev et al., 2016). Detailed geochemical characterization of KMSZ is lacking. The available geochemical data from the magmatic suite indicates a subduction-related arc magmatic origin, while the associated metasedimentary rocks are interpreted as volcano-sedimentary trench deposits, likely formed in an active continental margin setting (Amaldev et al., 2016).

3. Petrography

The charnockites used here in *sensu lato* sense (after Streckeisen, 1974; Frost and Frost, 2008), to denote orthopyroxene-bearing granitoids ranging from tonalitic (enderbitic) to granitic (charnockitic) compositions. All the charnockites studied here from the WDC, CB and KMSZ are composed of orthopyroxene±clinopyroxene–plagioclase–quartz–K-feldspar. They are mostly coarse to medium-grained non-garnetiferrous charnockites.

In the southern WDC, they occur as small bands elongated in a NNW–SSE direction (Fig. 2). They are mostly medium-grained, equigranular non-garnetiferous charnockites with well-developed foliation (Fig. 3a, b). These equigranular rocks are mainly composed of orthopyroxene ± clinopyroxene + plagioclase + quartz + K-feldspar ± biotite ± hornblende (Fig. 4a–c). The mafic rich variety contains a lot of hornblende and biotite that defines the foliation (Fig. 4b) where orthopyroxene is replaced by hornblende at places (Fig. 4b). Biotite occurs as individual grains as well as alteration product (Fig. 4c). Triple junctions sharing straight phase boundaries among different minerals attest to high-T annealing by grain-boundary area reduction (Fig. 4a). Quartz commonly shows undulose extinction (Fig. 4a, c).

The charnockite from the CB are coarse grained and massive in nature (Fig. 3c, d). They are composed of orthopyroxene + plagioclase + quartz + K-feldspar ± biotite ± hornblende (Fig. 4d-f). At places the orthopyroxene retrogressed to biotite (Fig. 4e). Locally the orthopyroxenes are replaced by amphibole+quartz corona (Fig. 4f, g). Chessboard twinning is a common feature in most of the quartz grains (Fig. 4h). Triple junctions with straight phase boundaries between different minerals indicate high-temperature annealing driven by the reduction of grain-boundary area (Fig. 4d, e).

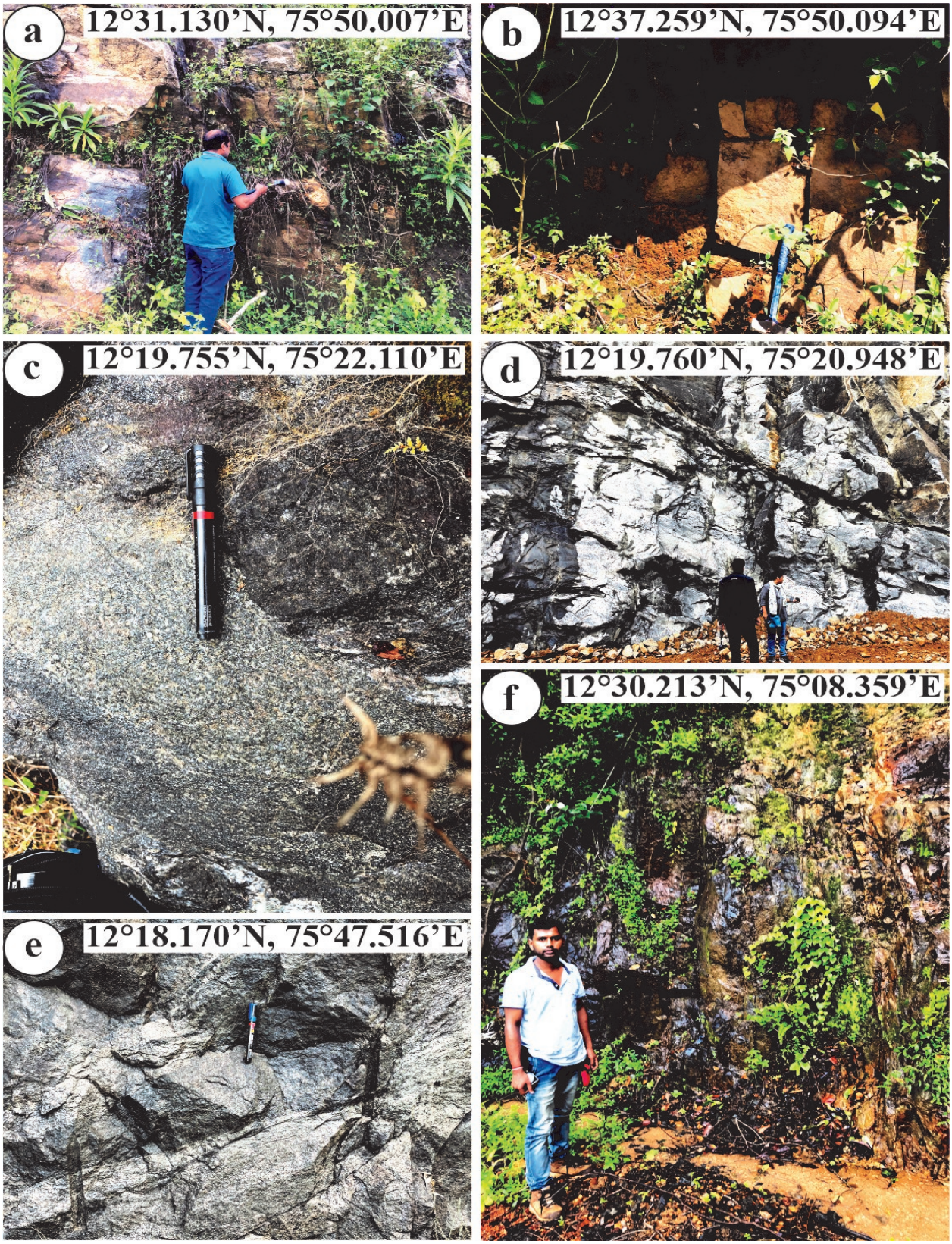

Fig. 3. Field photographs showing the charnockites from the Western Dharwar Craton (a, b), Coorg Block (c, d), and Kasargod–Mercara Shear Zone (e, f). (a, b) General appearance of the charnockites from the Western Dharwar Craton; photo taken looking south. (c) Close up and (d) general appearance of the charnockite from the Coorg Block. Photo taken looking east in (d). (e) Close up and (d) general appearance of the charnockite from the Kasargod–Mercara Shear Zone; photo taken looking east in (f). Pen head (15 cm long) points north.

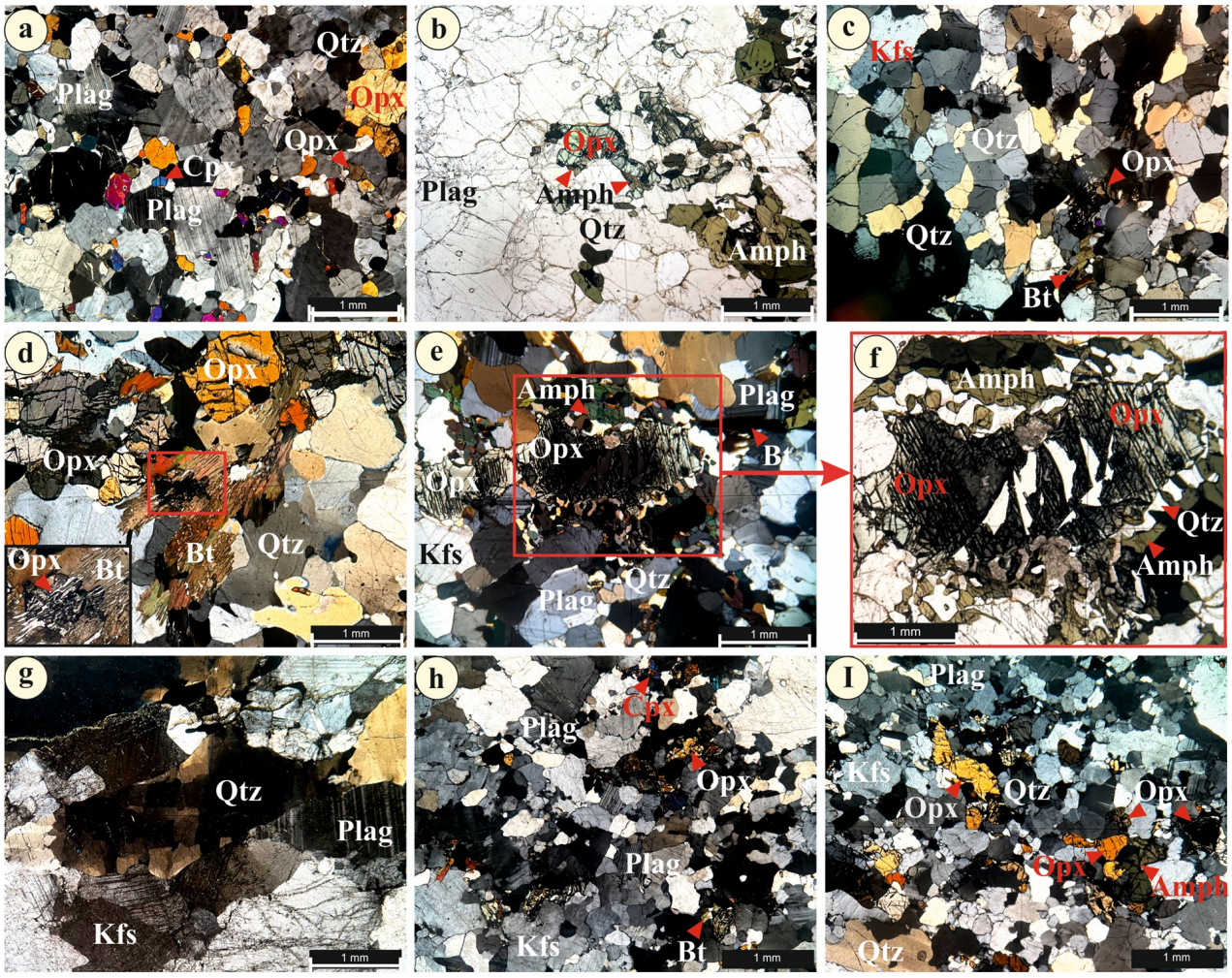

Fig. 4. Representative petrological images from the Western Dharwar Craton (a–c), Coorg Block (d–g), and Kasargod–Mercara Shear Zone (h–i). (a) Orthopyroxene–clinopyroxene–plagioclase associations typical of granulite-facies assemblages. (b) Orthopyroxene partially replaced by amphibole. (c) Orthopyroxene associated with quartz and K-feldspar, with localized replacement by biotite. (d) Charnockite showing orthopyroxene replaced by biotite; the red box highlights the retrogression, enlarged in the inset. (e) Coronitic and symplectitic intergrowths of orthopyroxene ± amphibole ± quartz, suggesting hydration reactions and partial breakdown of orthopyroxene. (f) Enlarged plane-polarized view of symplectitic and corona textures. (g) Coarse-grained quartz–K-feldspar–plagioclase intergrowth. (h, i) Samples from the Kasargod–Mercara Shear Zone characterized by granoblastic textures with plagioclase–quartz–K-feldspar–orthopyroxene assemblages. (h) Orthopyroxene retrogressed to biotite. (i) Orthopyroxene replaced by amphibole. Mineral abbreviations are after Kretz (1983).

The charnockite located along the KMSZ are small to medium-grained and are elongated parallel to the shear zone (Fig. 3e, f). They are composed of orthopyroxene ≫ clinopyroxene + plagioclase + quartz + K-feldspar (Fig. 4h, i). The grain size is smaller as compared to WDC and CB charnockites. Locally the orthopyroxenes are replaced by biotite (Fig. 4h) and hornblende (Fig. 4i). Dynamic recrystallization textures like bulge nucleation due to grain boundary migration recrystallization produced serrated grain boundaries between the minerals (Fig. 4h, i). Quartz shows undulose extinction (Fig. 4h, i). Subgrains are commonly observed (Fig. 4h).

4. Geochemistry

Total 17 samples (sample locations in Fig. 2) were selected for geochemical analysis. Out of these, six were from the WDC (MD-61, MD-63, MD-65, MD-67, MD-71 and MD-73), five were from the KMSZ (MD-7, MD-53, KG-39, KG-84 and KG-89) and six were from the CB (MD-86A, KG-46, KG-74A, KG-81B, WY-32A and WY-39). Each sample (weighing around 4 kg) was cleaned, crushed, and powdered to 200 mesh in a vibrating cup-mill at the Department of Earth and Atmospheric Sciences, National Institute of Technology Rourkela, India. The powdered samples were then dried in an oven at 110 °C overnight to

remove any adsorbed moisture (H_2O^-). After that, the weight loss on ignition (LOI) was determined by heating the powders at 950 °C in platinum crucibles. For preparing pressed pellets 7 g of the dry sample powders were mixed with 1 g of methyl cellulose binder using an Insmart XRF 40 hydraulic press with a maximum load of 20 tonnes. The major elements analyses were performed on a Rigaku ZSX Primus IV sequential wavelength dispersive X-Ray Fluorescence (XRF) spectrometer (4 kW) at the Department of Earth Sciences, Indian Institute of Technology Bombay, India. For calibrating the instrument, standards from the U. S. Geological Survey (BCR-2, BHVO-2 and W-2a) and the Geological Survey of Japan (JB-1b, JGb-2) were used. Two reference standards, i.e., QLO and DGH were used during the analysis. The analytical uncertainties are within ±2% for major elements. The major element chemical compositions and LOI values are presented in Table 1. Comparative geochemical data are provided in Table 2. The relevant geochemical plots are in Figs. 5–8.

4.1. Geochemical variations: Western Dharwar Craton

The charnockites of the WDC show silica (SiO_2) content ranging from 66.70 to 70.81 wt.%. The concentration of mafic oxides varies across the samples, with FeO content between 2.71 and 8.05 wt.%, MgO ranging from 0.58 to 2.19 wt.%, CaO from 2.85 to 3.59 wt.%, and TiO_2 between 0.24 and 0.95 wt.% (Table 1). Geochemical trends observed in the major oxides display a consistent negative correlation with increasing SiO_2 for MgO, FeO, CaO, TiO_2 and P_2O , (Fig. 5b, c, f, g, h). In contrast, oxides such as Al_2O , K_2O, and Na_2O show more scattered distributions relative to SiO_2 (Fig. 5a, d, e) (Frost et al., 2001).

In the TAS diagram by Middlemost (1994), all the charnockites from the WDC fall in the diorite to granodiorite composition field (Fig. 6a, b). Whereas in the normative feldspar differentiation diagram of O'Connor (1965), the charnockites extend into tonalite, trondhjemite and granodiorites fields (Fig. 6c). Classification based on the Fe* (FeO_{total}/FeO_{total}+MgO) index (Frost et al., 2001) places all the WDC charnockite samples within the ferroan field (Fig. 6d). The modified alkali-lime index (MALI) plotted as SiO_2 vs. Na_2O + K_2O–CaO (Frost et al., 2001), demonstrates a slight increase with rising silica content (Fig. 6e). Based on MALI values, the majority of WDC charnockites fall within the calcic to calc-alkalic fields, with most samples following a calcic trend (Fig. 6e). The K_2O/Na_2O ratio in the WDC charnockites averages approximately 0.37. The aluminum saturation index (ASI), as defined by Shand (1943), indicates that most charnockite samples are metaluminous, with only one sample falling into the peraluminous field (Fig. 6f).

4.2. Geochemical variations: Coorg Block

The charnockites of the CB exhibit a range of silica (SiO_2) contents, varying from 68.70 to 75.61 wt.%. The mafic oxides in these rocks are present in relatively low to moderate amounts, with FeO ranging between 1.87 and 3.91 wt.%, MgO between 0.26 and 0.77 wt.%, CaO from 2.99 to 4.83 wt.%, and TiO_2 varying from 0.12 to 1.08 wt.% (Table 1). Geochemical variation diagrams for major oxides demonstrate a coherent negative correlation between SiO_2 and Al_2O , FeO, CaO, TiO_2, and P_2O (Fig. 5a, c, f, g, h). In contrast, Na_2O and K_2O show considerable scatter when plotted against silica (Fig. 5d, e). Interestingly, MgO displays minimal variation across the samples.

The TAS diagram (Middlemost, 1994) shows that all the charnockites from the CB fall in the granodiorite to granitic composition field (Fig. 6a, b). Whereas in the normative feldspar differentiation diagram of O'Connor (1965), the charnockites straddle between tonalite to trondhjemite fields (Fig. 6c). Based on the Fe* index classification (Frost et al., 2001), three of the CB charnockite samples fall within the ferroan field, and samples with higher silica content plot near the magnesian-ferroan boundary (Fig. 6d). The Modified Alkali-Lime Index (MALI) (Frost et al., 2001), plotted against silica content, exhibits notable scatter in the CB charnockites, (Fig. 6e). Despite this scattering, all samples fall within the calcic field (Fig. 6e). The average K_2O/Na_2O ratio for the CB charnockites is approximately 0.14 (Tables 1, 2). The Aluminium Saturation Index (ASI; Shand, 1943) indicates that the CB charnockites are predominantly metaluminous (Fig. 6f).

4.3. Geochemical variations: Kasargod–Mercara Shear Zone

The charnockites of the KMSZ exhibit silica (SiO_2) content ranging from 69.68 to 74.16 wt.%. The concentrations of mafic oxides show moderate

Table 1. Major element compositions of charnockites from the Western Dharwar Craton (WDC), Kasargod Mercara Shear Zone (KMSZ) and Coorg Block (CB).

Western Dharwar Craton						
Oxides (Wt.%)	**MD-61**	**MD-63**	**MD-65**	**MD-67**	**MD-71**	**MD-73**
SiO_2	69.52	70.73	66.7	70.81	71.1	68.31
TiO_2	0.73	0.24	0.89	0.95	0.55	0.92
Al_2O_3	13.91	15.5	13.88	13.75	13.44	14.32
Fe_2O_3	4.84	2.44	5.92	4.27	4.6	7.25
MnO	0.06	0.05	0.06	0.05	0.06	0.07
MgO	1.45	0.58	2.19	1.11	1.27	1.11
CaO	3.22	2.85	3.47	2.85	3.36	3.59
Na_2O	4.94	5.96	4.16	4.15	4.28	3.92
K_2O	1.26	1.54	1.75	1.78	1.31	2.18
P_2O_5	0.15	0.12	0.21	0.13	0.12	0.3
LOI	1.18	1.5	1.01	0.97	0.77	1.25
Total	101.26	101.5	100.24	100.82	100.86	103.22
K_2O/Na_2O	0.26	0.26	0.42	0.43	0.31	0.56
Coorg Block						
Oxides (Wt.%)	**MD-86A**	**KG-46**	**KG-74A**	**KG-81B**	**WY-32A**	
SiO_2	68.7	70.2	71.66	69.27	75.61	
TiO_2	1.08	0.41	0.26	0.23	0.17	
Al_2O_3	15.07	14.82	16.15	16.3	11.14	
Fe_2O_3	3.52	3.4	1.87	2.52	1.95	
MnO	0.22	0.03	0.03	0.03	0.02	
MgO	0.26	0.63	0.66	0.77	0.6	
CaO	4.83	2.99	4.55	3.67	3.38	
Na_2O	4.37	5.58	5.02	5.15	4.75	
K_2O	0.62	0.68	0.39	0.65	1.18	
P_2O_5	0.32	0.19	0.1	0.08	0.08	
LOI	1.25	0.68	1.09	0.93	0.82	
Total	100.25	99.61	101.78	99.6	99.7	
K_2O/Na_2O	0.14	0.12	0.08	0.13	0.25	
Kasargod–Mercara Shear Zone						
Oxides (Wt.%)	**WY-39**	**MD-7**	**MD-53**	**KG-39**	**KG-84**	**KG-89**
SiO_2	74.80	74.16	69.68	70.41	69.90	71.38
TiO_2	0.12	0.26	1.50	0.75	1.42	0.28
Al_2O_3	12.63	14.05	14.34	14.71	14.02	15.62
Fe_2O_3	1.68	4.92	4.29	3.78	4.15	1.78
MnO	0.01	0.05	0.18	0.04	0.10	0.03
MgO	0.62	1.65	2.54	1.70	2.90	1.60
CaO	3.06	0.70	3.36	3.03	2.23	2.77
Na_2O	5.28	1.58	2.79	4.75	4.60	6.26
K_2O	0.52	0.85	0.14	0.53	0.77	1.15
P_2O_5	0.08	0.03	0.19	0.14	0.50	0.04
LOI	0.48	0.82	0.24	0.94	0.69	0.53
Total	99.28	99.08	99.24	100.77	101.29	101.43
K_2O/Na_2O	0.10	0.54	0.05	0.11	0.17	0.18

Table 2. Comparison of geochemical data between charnockites from the Western Dharwar Craton (WDC), Coorg Block (CB) and Kasargod–Mercara Shear Zone (KMSZ).

	WDC		**CB**		**KMSZ**	
Geochemical Classes	**Range**	**Average**	**Range**	**Average**	**Range**	**Average**
SiO_2 (wt %)	66.70–71.10	69.53	68.70–75.61	71.71	69.68–74.16	71.11
K_2O/Na_2O	0.26–0.56	0.37	0.08–0.25	0.14	0.05–0.54	0.21
ASI	0.02–0.08	0.05	0.01–0.08	0.03	0.02–0.17	0.09
Fe#	0.75–0.88	0.81	0.75–0.94	0.81	0.55–0.77	0.66
$Na_2O+K_2O–CaO$	2.22–4.66	2.98	0.17–3.28	1.95	0.43–4.64	2.26
$Na_2O+K_2O+MgO+FeO+TiO_2$	11.03–16.19	13.63	8.40–11.09	9.44	9.80–14.31	11.80
$(Na_2O+K_2O)/(FeO+MgO+TiO_2)$	2.79–3.98	3.32	2.62–3.84	3.21	2.35–5.62	4.37
$Al_2O_3+FeO+MgO+TiO_2$	19.03–24.40	21.56	14.08–20.32	18.09	19.46–23.14	21.67
$Al_2O_3/(FeO+MgO+TiO_2)$	1.42–4.39	2.18	2.87–5.39	4.04	1.57–4.06	2.28

variability, with FeO ranging from 1.97 to 5.47 wt.%, MgO between 1.60 and 2.90 wt.%, CaO from 0.70 to 3.36 wt.%, and TiO_2 between 0.26 and 1.50 wt.% (Table 1). Geochemical trends observed in the KMSZ

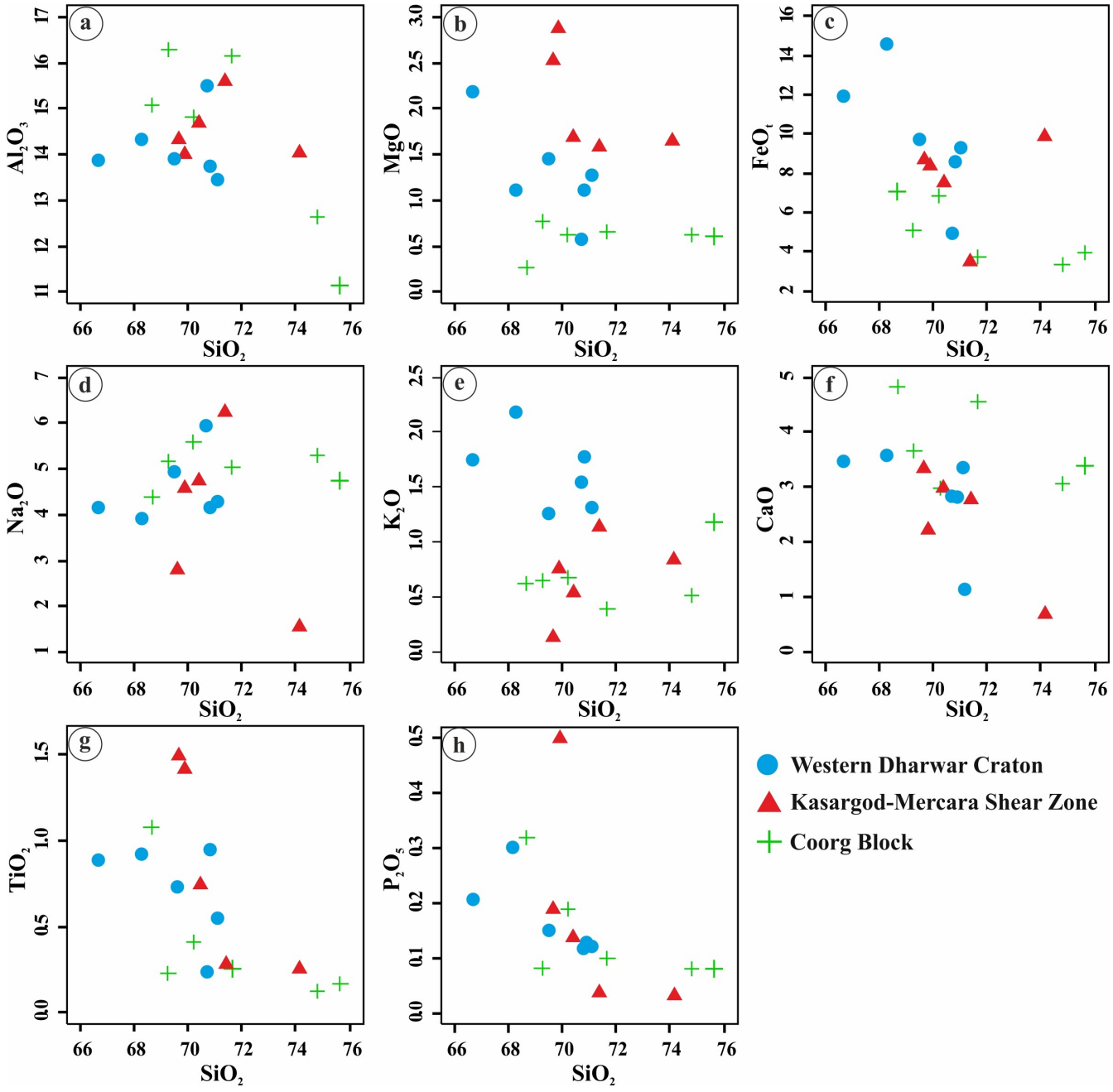

Fig. 5. Harker variation diagrams for major element oxides vs. SiO_2 (in wt.%) from the Western Dharwar Craton, Coorg Block and Kasargod–Mercara Shear Zone.

charnockites reveal a coherent negative correlation between SiO_2 and several major oxides, including Al_2O_3, MgO, FeO, CaO, TiO_2, and P_2O (Fig. 5a–c, f–h). In contrast, Na_2O and K_2O display scattered distributions relative to SiO_2 (Fig. 5d, e).

The TAS diagram (Middlemost, 1994) shows that all charnockites from the KMSZ fall within the granodiorite composition field (Fig. 6a, b), whereas in the normative feldspar differentiation diagram (O'Connor, 1965), the charnockites straddle the tonalite-trondhjemite fields (Fig. 6c). Tectonic discrimination diagrams using the Fe* index (Frost et al., 2001) indicate that all charnockite samples from the KMSZ fall within the magnesian field (Fig. 6d). The Modified Alkali-Lime Index (MALI) (Frost et al., 2001) shows a clear increase with rising silica content in the KMSZ charnockites (Fig. 6e). Based on this index, the samples are classified as calcic in composition (Fig. 6e). The average K_2O/Na_2O ratio in the KMSZ charnockites is approximately 0.21 (Tables. 1, 2). The Aluminium Saturation Index (ASI; Shand, 1943) shows that most of the

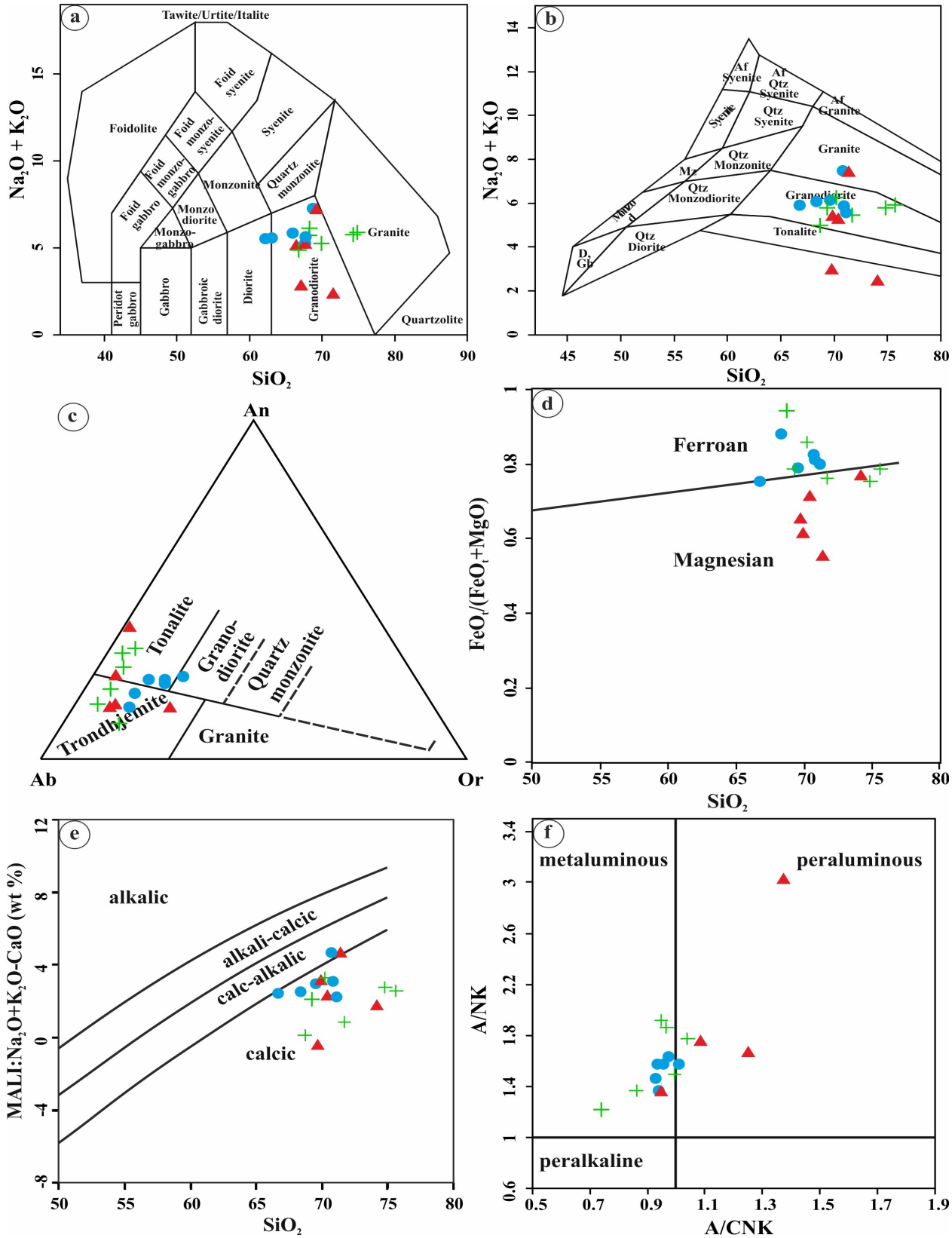

Fig. 6. (a–b) TAS diagram of Na_2O+K_2O vs SiO_2 after Middlemost (1985, 1994), (c) Feldspar triangle (An–Ab–Or), (d) $FeO_t/(FeO_t+MgO)$ vs. SiO_2 showing ferroan and magnesian nature of charnockites; the boundary is after Frost et al. (2001), (e) Modified alkali-lime index (MALI) plots of $Na_2O/(K_2O–CaO)$ vs. SiO_2 (Frost et al., 2001), and (f) Molar $Al_2O_3/(Na_2O+K_2O)$ vs. alumina-saturation index (ASI = molar $Al_2O_3/[CaO + Na_2O + K_2O]$) (Frost and Frost, 2008). Symbols are same as in Fig. 5.

charnockite samples fall within the peraluminous-metaluminous field (Fig. 6f).

Major element systematics serve as first-order proxies for magmatic lineages, yet their interpretation in granulite-facies terranes can be influenced by metamorphic re-equilibration. Although trace element and isotopic datasets are more discriminative, this study aims to establish compositional trends that complement prior trace-element studies (e.g., Santosh et al., 2015).

5. Discussion

The petrographic studies of charnockites from the southern WDC, KMSZ and CB indicates high-T deformation from the granoblastic textures, dynamic recrystallization of minerals, formation of triple junctions etc. (Fig. 4a, d, g, h). Textural relationships, such as polygonal granoblastic matrices and annealed quartz-feldspar intergrowths, suggest equilibration under granulite-facies conditions, comparable to P-T estimates from Yang et al. (2023) for the CB. The Southern WDC charnockites are foliated mafic rocks showing evidence of both high-temperature annealing and hydration retrogression, particularly in their mafic-rich variants. The development of hornblende and biotite, along with quartz deformation textures, suggests moderate ductile deformation under retrograde conditions (Fig. 4b, c). In contrast, the CB charnockites are massive and coarse-grained, preserving a dominantly dry high-temperature mineral assemblage. Features such as chessboard twinning in quartz and limited biotite retrogression point to high-T strain and minor fluid interaction during cooling and exhumation (Fig. 4e, f). The KMSZ charnockites display the most intense deformation-related overprint. Although originally high-temperature rocks, they have been strongly modified by shear zone processes, including dynamic recrystallization, quartz subgrain development, and grain-boundary migration textures (Fig. 4g, h). The absence of biotite and minimal hornblende replacement suggests restricted retrogression despite extensive deformation.

5.1. Petrogenetic constraints and source characteristics

The charnockites of the KMSZ and across the shear zone exhibit a range of silica (SiO_2) content indicating their felsic to intermediate composition. Geochemical trends observed in the major oxides display a consistent negative correlation with increasing SiO_2 for MgO, FeO, CaO, TiO_2, and P_2O , indicating progressive removal of mafic phases during magmatic differentiation (Fig. 5b, c, f–h). In contrast, oxides such as Al_2O_3, Na_2O, and K_2O show more scattered distributions relative to SiO_2, which may reflect variable degrees of crustal interaction or heterogeneity in the source composition, consistent with the observations of Frost et al. (2001) (Fig. 5a, d, e). Interestingly, in CB MgO displays minimal variation across the samples, indicating limited mafic mineral fractionation or a homogeneous mafic source. Classification based on the Fe* index (Frost et al., 2001) places all WDC charnockite samples within the ferroan field (Fig. 6d), whereas all the samples from the KMSZ fall within the magnesian field (Fig. 6d). The WDC charnockites may have formed from iron-rich melt consistent with evolved magmatic conditions that may involve significant crustal contribution (Frost and Frost, 2008; Rajesh and Santosh, 2012). The KMSZ charnockites may reflect mantle-influenced magmatism subsequently modified by deformation and fluid-assisted processes within the shear zone. The CB charnockites show ferroan to magnesian signatures indicating a heterogeneous source region or magma mixing between crustal and mantle-derived components (Frost et al., 2001). The modified alkali-lime index demonstrates a slight increase with rising silica content, reflecting progressive alkali enrichment in all the studied charnockites (Frost et al., 2001) (Fig. 6e). Based on MALI values, all the charnockites fall within the calcic fields suggesting a magmatic affinity with a dominant calcium-rich signature. Such calcic affinity is commonly observed in arc-related magmatic suites but does not uniquely constrain mantle versus crustal sources (Pearce et al., 1984). Furthermore, these features are broadly consistent with magmatism in active continental margin settings, where magmas are commonly generated in subduction-influenced regimes (Pitcher, 1987). The alumina saturation index (ASI), as defined by Shand (1943), indicates that most charnockite samples from the WDC and CB are metaluminous, while the KMSZ charnockites are mostly peraluminous to metaluminous (Fig. 6f). The metaluminous compositions are consistent with derivation from igneous protoliths or mantle-influenced lower crustal sources with limited crustal contamination in WDC and CB. In contrast, peraluminous to metaluminous compositions in the

KMSZ charnockites may indicate involvement of continental crustal material, possibly through partial melting, magma mixing, or advanced fractionation processes. The peraluminous nature also may reflect fluid–rock interaction and metamorphic modification along shear zones, highlighting the tectonic influence on magma evolution and emplacement processes in the KMSZ.

The geochemical characteristics of charnockites from the WDC, KMSZ, and CB reflect varied petrogenetic histories across the southern Indian granulite terrane. Most of the studies on charnockites from the WDC is on Kabbaldurga region where the charnockite occur as patches and veins (Janardhan et al., 1979; Katz, 1989; Bhattacharya and Sen, 2000). The studies from small individual charnockite bodies within the WDC are missing. Most of the existing studies suggest that the transformation from amphibolite- to granulite-facies assemblages was triggered by CO_2-rich fluids, likely derived from deeper granulitic crust (Stähle et al., 1987; Santosh et al., 2004; Ravindra Kumar and Venkatesh Raghavan, 1992, Srikantappa et al., 1992, Santosh and Tsunogae, 2003). Using the geochemical data from the Kabbaldurga region Bhattacharya and Chaudhary (2013) argued that the patchy charnockites are not formed by the in-situ transformation from amphibolite facies gneisses. According to them, the charnockitic leucosomes at mafic granulite margins and charnockitic veins within mafic granulite enclaves are the result of dehydration partial melting in mafic rocks. From the present study the major element oxide trends with respect to SiO_2 in the WDC charnockites indicates fractionation of mafic minerals during magma differentiation and later crustal contamination consistent with earlier studies on the Closepet granite and Peninsular Gneiss Complex (Taylor et al., 1984; Moyen et al., 2003). Similar to the charnockites studied here the pegmatitic charnockites from Kabbalaldurga correspond to tonalite, trondhjemite and granite composition whereas non-pegmatitic charnockite from Kabbaldurga and Kodamballi, fall in the field of tonalite (Bhattacharya and Sen, 2000). The present study suggests that the WDC charnockites were derived from relatively iron-rich melts, possibly associated with post-orogenic settings involving crustal input. Geochemical characteristics further indicate contributions from mantle-influenced and/or lower crustal sources, consistent with derivation from igneous protoliths.

The charnockites from the CB show tonalitic-trondhjemitic affinity and can be classified as intermediate type (Rajesh and Santosh, 2004; Tomson et al., 2006; Rajesh, 2007). They have distinct geochemical signatures such as low K_2O/Na_2O ratio, predominantly magnesian, metaluminous, and having calcic affinity similar to that of fractionated I-type granites (Rajesh, 2007). Previous studies on charnockites from the CB suggest that they are silicic to intermediate charnockites showing arc-related signature and magma generation within a convergent margin setting (Yang et al., 2023). The geochemical features from the existing literature suggests an initial partial melting of hydrous basaltic magma and later fractionation (Rajesh, 2007; Yang et al., 2023). From the present study, the minimal variation in MgO, combined with transitional ferroan-magnesian and metaluminous signatures, suggests that the source magma was likely derived from a mantle or mafic lower crustal origin, with limited fractional crystallization and minimal crustal contamination. These features are characteristic of magmas with an I-type affinity, and are broadly consistent with subduction-related magmatic signatures or possibly late- to post-collisional settings, which is consistent with the previous observations.

The limited studies from the KMSZ by Amaldev et al. (2016) suggest that the metaluminous nature, lower K_2O/Na_2O ratios, and similarity to high Ba–Sr granitoids provide evidence for the magmatic parentage for the charnockites. In contrast, in the present study, the charnockites with magnesian and calcic signatures are consistent with derivation from mantle-influenced or mafic lower crustal sources, typical of I-type magmas formed in subduction-related settings. However, the metaluminous to peraluminous characteristics imply magma mixing or source hybridization, potentially influenced by shear zone-controlled melt migration and crust-mantle interaction during magmatic emplacement. The KMSZ charnockites also show negative trends for major mafic oxides but exhibit greater variability in alkali elements, possibly due to metasomatic modification or partial melting of diverse crustal protoliths (Jayananda et al., 2006). Petrographic evidence, including myrmekitic textures, alignment of feldspars, and recrystallized quartz ribbons, suggests that melt migration was locally guided by ductile shearing along the KMSZ. Thus, the KMSZ likely acted as a rheologically weak channel that facili-

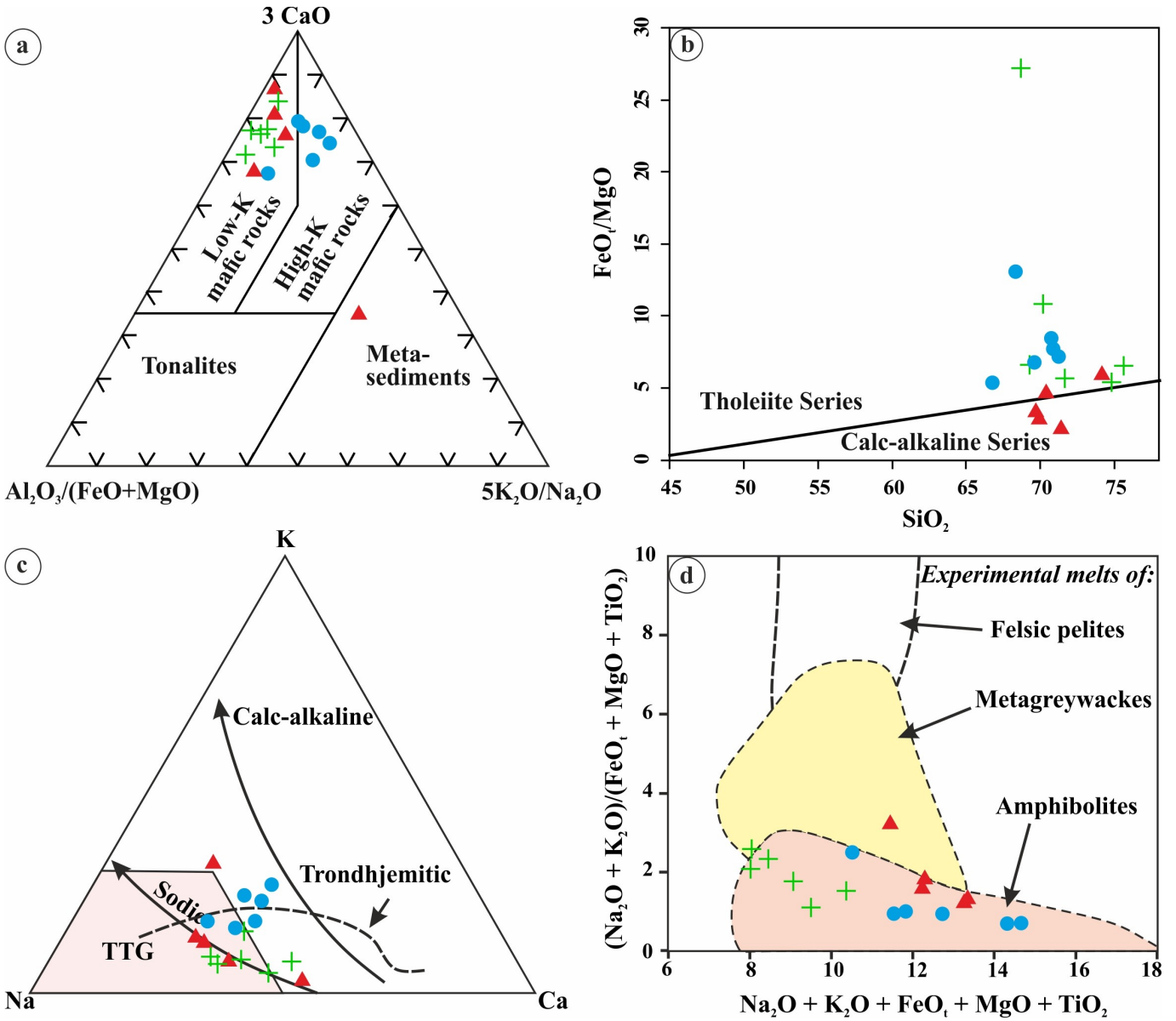

Fig. 7. Source diagrams (a) $3CaO–Al_2O_3/(FeO+MgO)–5K_2O/Na_2O$ and (b) SiO_2 vs FeO/MgO (after Miyashiro, 1974). (c) K–Na–Ca triangular diagram showing the TTG trend after Barker and Arth (1976). (d) $[Al_2O_3/(FeO_t+MgO+TiO_2)]$ vs. $[Al_2O_3+FeO_t+MgO+TiO_2]$ after Patiño Douce (1999). Symbols are same as in Fig. 5.

tated melt migration and was subsequently reactivated during late-stage transpressional deformation. Petrographic evidence such as chessboard twinning, quartz subgrain formation, and dynamic recrystallization in KMSZ charnockites indicates deformation under granulite-facies conditions. These features suggest syn- to post-emplacement ductile deformation consistent with dextral transpression along the KMSZ (Rekha et al., 2014). In contrast, annealing textures in the WDC and CB charnockites reflect static recrystallization during cooling and metamorphic overprinting. Overall, deformation and magma emplacement are closely linked, with shear zone dynamics controlling both melt migration and subsequent deformation history.

The plot based on Laurent et al. (2014), is used to infer source characteristics of charnockites based on major element ratios (Fig. 7a). The WDC charnockites plot within the high-K mafic rocks field, suggesting derivation from mafic lower crustal or mantle-influenced sources with high-K characteristics, consistent with, metaluminous, tholeiitic signatures of the WDC (Fig. 7b). The CB and KMSZ charnockites fall in the low-K mafic rock field. The CB charnockites with a metaluminous, tholeiitic signatures and low-K mafic signatures suggest derivation from a depleted

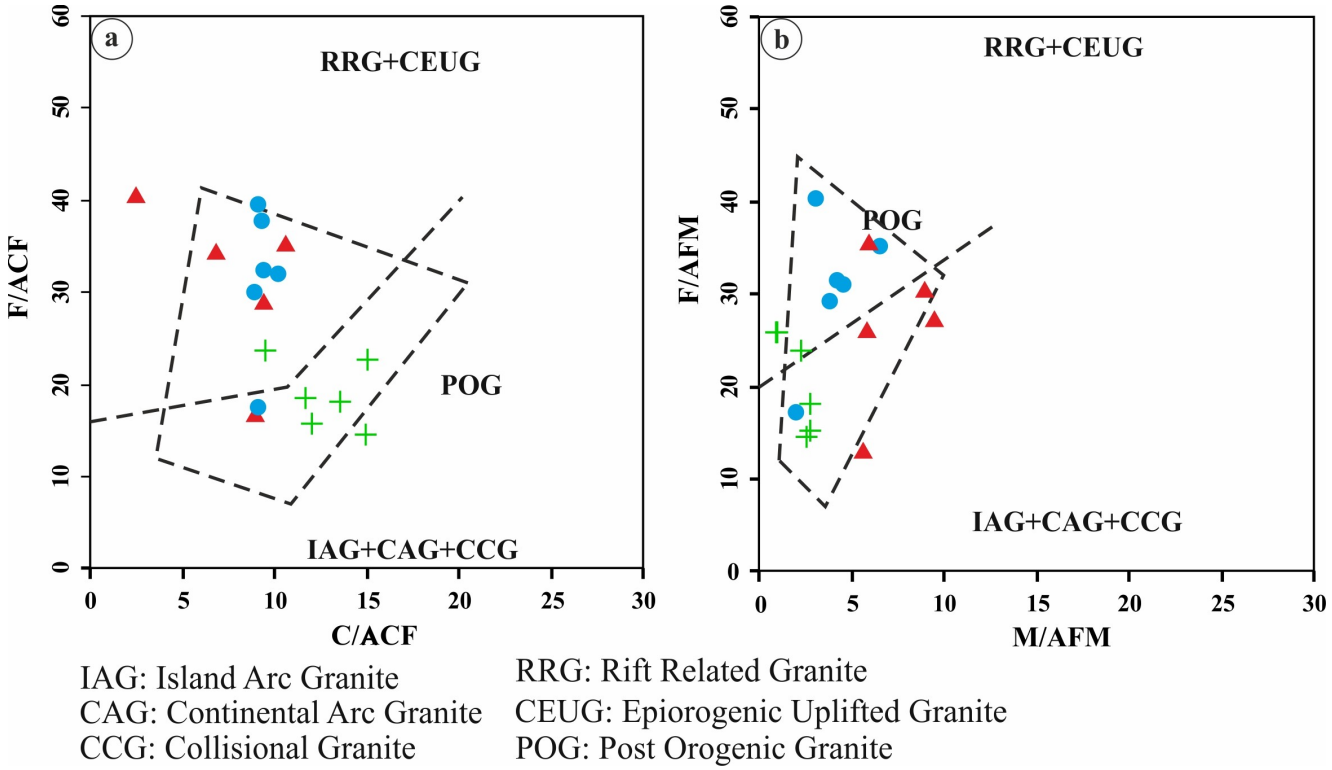

Fig. 8. Granite tectonic discrimination diagrams (a) C/ACF vs F/ACF, (b) M/AFM vs F/AFM (after Maniar and Piccoli, 1989). Symbols are the same as in Fig. 5.

mafic lower crust or mantle-influenced source with limited potassium enrichment. Such characteristics are typical of high-grade granulitic protoliths formed under dry, high-temperature conditions. Whereas the KMSZ charnockites with peraluminous to metaluminous, calc-alkaline magma signature are consistent with high-temperature protoliths that may have formed in subduction-related or post-collisional environments, involving partial melting of mafic protoliths. In the K–Na–Ca ternary diagram (Fig. 7c) a predominant Archaean TTG affinity is noticed, where the CB and KMSZ samples following the sodic TTG evolution trend of Luais and Hawkesworth (1994) and the WDC charnockites are following the trondhjemitic TTG trend of Barker and Arth (1976). In the [$(Na_2O+K_2O)/(FeO_t+MgO+TiO_2)$] vs. [$Na_2O+K_2O+FeOtot+MgO+TiO_2$] diagrams (Patiño Douce, 1999), (Fig. 7d) most of the studied charnockites fall in the amphibolite and metabasalt-metatonalite field indicate the partial melting-induced magmatic differentiation during their formation. The peraluminous nature of the KMSZ charnockites likely represents late-stage fluid-rock interaction during deformation, rather than direct evidence of shear-induced melting, preserving the tectonic significance without overinterpretation.

Published U–Pb zircon ages for WDC charnockitic magmatism cluster around 2.56–2.60 Ga (Jayananda et al., 2013a,b), whereas CB granitoids crystallized between 2.90–3.10 Ga (Santosh et al., 2015; Basak et al., 2023). The KMSZ records younger reactivation at ca. 2.45 Ga (Rekha et al., 2014). These temporal patterns indicate progressive crustal accretion and subsequent transpressional reworking along the WDC–KMSZ–CB boundary.

5.2. Tectonic settings

Major elements are broadly used as discrimination tools to differentiate between various tectonic settings of charnockites. According to major element geotectonic dis-crimination diagrams (Fig. 8a, b) the compositions of the WDC, CB and KMSZ charnockites are broadly compatible with post-orogenic or evolved magmatic settings (Maniar and Piccoli, 1989). This is supported by the major element geochemistry from the three crustal domains. The WDC charnockites with high-K mafic rock affinity, metaluminous, and tholeiitic signatures, are consistent with evolved magmatic sources that may be related to post-collisional tectonic conditions. The CB charnockites exhibit metaluminous, tholeiitic geochemical signatures and

with low-K mafic rock affinity are broadly consistent with mantle-influenced magmas emplaced in subduction-related settings, although this interpretation requires further support from trace element and isotopic data. The KMSZ charnockites exhibit peraluminous to metaluminous compositions and display calc-alkaline magmatic signatures suggest derivation from mixed crustal-mantle sources, possibly associated with convergent margin processes and subsequent deformation within the shear zone. Similar to the observations made in this study the recent studies on the geochemical characteristics of charnockite from the CB and KMSZ also support a subduction related origin (Amaldev et al., 2016; Yang et al., 2023). Basak et al. (2023) proposed that Coorg Block and adjoining shear zones record crustal thickening and partial melting under convergent settings, integrating both subduction and collisional features. It is important to note that tectonic interpretations based solely on major element geochemistry provide only first-order constraints. Integration with trace element and isotopic datasets is required to robustly constrain the geodynamic setting.

6. Conclusions

The petrographic and major element geochemical data of charnockites from the WDC, CB, and KMSZ reveal direct evidence for the distinct petrogenetic histories and tectonic settings across the KMSZ. The metamorphic imprints likely record overprinting associated with the late Neoarchean collisional phase, coinciding with the regional high-temperature conditions that affected the KMSZ and adjacent domains. The WDC charnockites, with high-K, ferroan, metaluminous, and tholeiitic characteristics, likely formed from evolved, crustally influenced melts consistent with post-collisional or late-orogenic settings. In contrast, the CB charnockites display low-K, magnesian, metaluminous compositions with calcic affinities and are consistent with mantle-influenced magmas that may have been emplaced in subduction-related arc environments. The KMSZ charnockites, exhibiting peraluminous to metaluminous, calc-alkaline compositions and strong deformation fabrics, suggest formation in a convergent margin setting, with subsequent modification by deformation and crust-mantle interaction within the shear zone. Overall, these results highlight the interplay of mantle input, crustal assimilation, and tectonic regime in shaping the magmatic and metamorphic evolution of the southern part of the WDC, CB and the shear zone between them during the late Archean to early Proterozoic.

Acknowledgements

This work forms part of the doctoral dissertation of SN, who was supported by the research fellowship from DST-SERB (Project code: SR/19/ER-12). SR acknowledges the financial support provided by DST-SERB (Project code: SR/19/ER-12). The funding agency had no role in the design or execution of this study. The editorial handling by Prof. A. P. Pradeepkumar is gratefully acknowledged.

CRediT statement

S Rekha: Conceptualization, supervision, funding acquisition, investigation, validation, visualization, review, editing. **S.Nanda:** Data curation, formal analysis, investigation, validation, visualization, writing original draft, review and editing

Conflict of interest

The authors declare that they have no known competing financial interests or personal relationships that could have appeared to influence the work reported in this paper.

Data availability

All the data generated during this study are incorporated within the article.

References

Amaldev, T., Santosh, M., Tang, L., Baiju, K.R., Tsunogae, T., Satyanarayanan, M., 2016. Mesoarchean convergent margin processes and crustal evolution: Petrologic, geochemical and zircon U–Pb and Lu–Hf data from the Mercara Suture Zone, southern India. *Gondwana Res* 37, 182–204,. https://doi.org/10.1016/j.gr.2016.05.017.

Anoop, K.S., Anilkumar, Y., Santosh, M., Yu, B., Joy, K.D., Kavyanjali, K.V., Sajinkumar, K.S., 2022. Magmatic and metamorphic evolution of a layered gabbro–anorthosite complex from the Coorg Block, southern India: implications for Mesoarchean suprasubduction zone processes. *Gondwana Res* 103, 105–134,. https://doi.org/10.1016/j.gr.2021.07.026.

Asha Manjari, K., Malur, K.S., 1997. Petrology of charnockites from the Coorg region, Karnataka. *J. Geol. Soc. India* 49, 121–132.

Barker, F., Arth, J.G., 1976. Generation of trondhjemitic–tonalitic liquids and Archean bimodal trondhjemite–basalt suites. *Geology* 4, 596–600,. https://doi.org/10.1130/0091-7613(1976)4.

Basak, S., Hasenstab, E., Bhowmik, S.K., Gerdes, A., Dasgupta, S., Münker, C., Ravindra Kumar, G., Chakraborty, S., 2023. Thermal and chemical evolution of an Archean collision zone: insights from P–T–t history of mafic granulites from the Coorg Block, S. India. *Journal of Petrology* 64(5), 026. https://doi.org/10.1093/petrology/egad026.

Beckinsale, R.D., Drury, S.A., Holt, R.W., 1980. 3360 m-yr. old gneisses from the south Indian Craton. *Nature* 283, 469–470. https://doi.org/10.1038/283469a0.

Bhattacharya, S., Chaudhary, A., 2013. Kabbaldurga charnockites revisited: Incipient growth or anatectic melt? *Natural Science* 5, 419–436. https://doi.org/10.4236/ns.2013.53055.

Bhattacharya, S., Sen, S.K., 2000. New insights into the origin of Kabbaldurga charnockites, Karnataka, South India. *Gondwana Res* 3, 489–506. https://doi.org/10.1016/S1342-937X(05)70756-5.

Chardon, D., Jayananda, M., J.-J, Peucat, 2011. Lateral constrictional flow of hot orogenic crust: Insights from the Neoarchean of south India, geological and geophysical implications for orogenic plateau. *Geochem. Geophys. Geosyst* 12(2). https://doi.org/10.1029/2010GC003398.

Chardon, D., Jayananda, M., Peucat, J..J., 2008. Precambrian continental strain and shear zone patterns: South Indian case. *J. Geophys. Res. Solid Earth* 113, B08402, 1–16. https://doi.org/10.1029/2007JB005299.

Chetty, T.R.K., Mohanty, D.P., Yellappa, T., 2012. Mapping of shear zones in the Western Ghats, Southwestern part of Dharwar Craton. *J. Geol. Soc. India* 79, 151–154. https://doi.org/10.1007/s12594-012-0023-1.

Dhoundial, D.P., Sarkar, D.K., Trivedi, J.R., Gopalan, K., Potts, P.J., 1987. Geochronology and geochemistry of Precambrian granitic rocks of Goa, southwest India. *Precambrian Res* 36, 287–302. https://doi.org/10.1016/0301-9268(87)90026-X.

Friend, C.R.L., Nutman, A.P., 1991. Shrimp U–Pb Geochronology of the Closepet Granite and Peninsular Gneiss, Karnataka, South-India. *Jour. Geol. Soc. India* 38, 357–368. https://doi.org/10.17491/jgsi/1991/380402.

Frost, B.R., Barnes, C.G., Collins, W.J., Arculus, R.J., Ellis, D.J., Frost, C.D., 2001. A geochemical classification for granitic rocks. *J. Petrol* 42, 2033–2048. https://doi.org/10.1093/petrology/42.11.2033.

Frost, B.R., Frost, C.D., 2008. On charnockites. *Gondwana Res* 13, 30–44,. https://doi.org/10.1016/j.gr.2007.07.006.

Harley, S.L., 1989. The origins of granulites: a metamorphic perspective. *Geol. Mag* 126(3), 215–247,. https://doi.org/10.1017/S0016756800022330.

Janardhan, A., Newton, R., Smith, J., 1979. Ancient crustal metamorphism at low pH2O: charnockite formation at Kabbaldurga, south India. *Nature* 278, 511–514,. https://doi.org/10.1038/278511a0.

Jayananda, M., Chardon, D., Peucat, J..J., Capdevila, R., 2006. 2.61 Ga potassic granites and crustal reworking in the western Dharwar craton, southern India: tectonic, geochronologic and geochemical constraints. *Precambrian Res* 150, 1–26,. https://doi.org/10.1016/j.precamres.2006.05.004.

Jayananda, M., Chardon, D., Peucat, J..J., Fanning, C.M., 2015. Paleo- to Mesoarchean TTG accretion and continental growth, western Dharwar craton, southern India: SHRIMP U-Pb zircon geochronology, whole-rock geochemistry and Nd-Sr isotopes. *Precambrian Res* 268, 295–322,. https://doi.org/10.1016/j.precamres.2015.07.015.

Jayananda, M., Kano, T., Peucat, J..J., Channabasappa, S., 2008. 3.35 Ga komatiite volcanism in the western Dharwar craton, southern India: constraints from Nd isotopes and whole rock geochemistry. *Precambrian Res* 162, 160–179,. https://doi.org/10.1016/j.precamres.2007.07.010.

Jayananda, M., Peucat, J..J., Chardon, D., Krishna Rao, B., F, Corfu, 2013a. Neoarchean greenstone volcanism, Dharwar craton, Southern India: Constraints from SIMS zircon geochronology and Nd isotopes. *Precambrian Res* 227, 55–76,. https://doi.org/10.1016/j.precamres.2012.05.002.

Jayananda, M., Tsutsumi, Y., Miyazaki, T., Gireesh, R.V., Kapfo, Kowe.u, Tushipokla, Hidaka, H., Kano, 2013b. Geochronological constraints on Meso-neoarchean regional metamorphism and magmatism in the Dharwar craton, southern India. *J. Asian Earth Sci* 78, 8–38,. https://doi.org/10.1016/j.jseaes.2013.04.033.

Katz, M.B., 1989. Charnockites in the Baking at Kabbaldurga? *J. Geol. Soc. India* 33(3), 215–217.

Kretz, R., 1983. Symbols for rock forming minerals. *Am. Mineral* 68, 277–279.

Laurent, O., Martin, H., Moyen, J.F., Doucelance, R., 2014. The diversity and evolution of late-Archean granitoids: evidence for the onset of "modern-style" plate tectonics between 3.0 and 2.5 Ga. *Lithos* 205, 208–235,. https://doi.org/10.1016/j.lithos.2014.06.012.

Luais, B., Hawkesworth, C.J., 1994. The generation of continental crust: an integrated study of crust-forming processes in the Archaean of Zimbabwe. *J. Petrol* v.35, 43–93,. https://doi.org/10.1093/petrology/35.1.43.

Maniar, P.D., Piccoli, P.M., 1989. Tectonic discrimination of granitoids. *Geol. Soc. Am. Bull* 101, 635–643.

Meen, J.K., Rogers, J.J.W., Fullagar, P.D., 1992. Lead isotopic compositions of the Western Dharwar Craton, Southern India: evidence for distinct Middle Archean terranes in a Late Archean Craton. *Geochim. Cosmochim. Acta* 56, 2455–2470,. https://doi.org/10.1016/0016-7037(92)90202-T.

Middlemost, E.A.K., 1985. *Magmas and Magmatic Rocks. An Introduction to Igneous Petrology.* Longman Group Ltd, London, New York.

Middlemost, E.A.K., 1994. Naming materials in the magma/igneous rock system. *Earth-Sci. Rev* 37, 215–224,. https://doi.org/10.1016/0012-8252(94)90029-9.

Miyashiro, A., 1974. Volcanic rock series in island arcs and

active continental margins. *Am. J. Sci* 274, 321–355. https://doi.org/10.2475/ajs.274.4.321.

Moyen, J.F., 2009. High Sr/Y and La/Yb ratios: The meaning of the "adakitic signature". *Lithos* 112, 556–574,. https://doi.org/10.1016/j.lithos.2009.04.001.

Moyen, J..F., Nedelec, A., Martin, H., Jayananda, M., 2003. Syntectonic granite emplacement at different structural levels: the Closepet granite, South India. *J. Struct. Geol* 25, 611–631,. https://doi.org/10.1016/S0191-8141(02)00046-9.

Naha, K., Srinivasan, R., Gopalan, K., Pantulu, G.V.C., Subba Rao, M.V., Vrevsky, A.B., Bogomolov, Y.E.S., 1993. The nature of the basement in the Archaean Dharwar craton of southern India and the age of the Peninsular Gneiss. *Proc. Ind. Acad. Sci. (Earth and Planetary Sciences)* 102, 547–556,. https://doi.org/10.1007/BF02871953.

Nutman, A.P., Chadwick, B., Krishna Rao, B., Vasudev, V.N., 1996. SHRIMP U–Pb zircon ages of acid volcanic rocks in the Chitradurga and Sandur Groups and granites adjacent to Sandur schist belt. *J. Geol. Soc. India* 47, 153–161,. https://doi.org/10.17491/jgsi/1996/470202.

O'Connor, J.T., 1965. *A Classification of Quartz-rich Igneous Rock Based on Feldspar Ratios*. volume 525B. US Geological Survey. URL: https://ci.nii.ac.jp/naid/10003543275.

Patiño Douce, A.E., 1999. What do experiments tell us about the relative contributions of crust and mantle to the origin of granitic magmas? *Geological Society, London, Special Publications* 168, 55–75. https://doi.org/10.1144/gsl.sp.1999.168.01.05.

Pearce, J.A., Harris, N.B.W., Tindle, A.G., 1984. Trace element discrimination diagrams for the tectonic interpretation of granitic rocks. *J. Petrol* 25, 956–983. https://doi.org/10.1093/petrology/25.4.956.

Peucat, J.J., Bouhallier, H., Fanning, C.M., Jayananda, M., 1995. Age of the Holenarsipur Greenstone-Belt: relationships with the surrounding gneisses (Karnataka, South India). *J. Geo* 103, 701–710,. https://doi.org/10.1086/629789.

Peucat, J..J., Jayananda, M., Chardon, D., Capdevila, R., Fanning, C.M., Paquette, J..L., 2013. The lower crust of the Dharwar Craton, Southern India: patchwork of Archean granulitic domains. *Precambrian Res* 227, 4–28,. https://doi.org/10.1016/j.precamres.2012.06.009.

Peucat, J..J., Mahabaleswar, B., Jayananda, M., 1993. Age of younger tonalitic magmatism and granulite metamorphism in the amphibolite–granulite transition zone of southern India (Krishnagiri area): comparison with older peninsular gneisses of Gorur- Hassan area. *J. Metamorph. Geol* 11, 879–888,. https://doi.org/10.1111/j.1525-1314.1993.tb00197.x.

Peucat, J..J., Vidal, Ph, Bernard-Griffiths, J., Condie, K.C., 1989. Sr, Nd and Pb isotopic systematics in the Archaean low-to-high-grade transition zone of southern India: synaccretion vs. post accretion granulites. *J. Geol* 97, 537–550,. https://doi.org/10.1086/629333.

Pitcher, W.S., 1987. Granites and yet more granites forty years on. *Geol. Rundsch* 76(1), 51–79,. https://doi.org/10.1007/BF01820573.

Praharaj, P., Rekha, S., 2022. Tectono-metamorphic evolution of the Trivandrum and Southern Madurai blocks in the Southern Granulite Terrane, south India: Correlation with south-central Madagascar. *Geol. Mag* 159, 1569–1600. https://doi.org/10.1017/S0016756822000413.

Raith, M., Hoernes, S., Klatt, E., Stähle, H.J., 1989. Contrasting mechanisms of charnockite formation in the amphibolite to granulite grade transition zones of Southern India, in: Bridgwater, D. (Ed.), *Fluid Movements — Element Transport and the Composition of the Deep Crust*. Springer, Dordrecht. volume 281 of *NATO ASI Series*. https://doi.org/10.1007/978-94-009-0991-5_3.

Rajesh, H.M., 2007. The petrogenetic characterization of intermediate and silicic charnockites in high-grade terrains: A case study from Southern India. *Contrib. Mineral. Petrol* 154, 591–606,. https://doi.org/10.1007/s00410-007-0211-y.

Rajesh, H.M., Santosh, M., 2004. Charnockitic magmatism in southern India. *J. Earth Syst. Sci* 113, 565–585,. https://doi.org/10.1007/BF02704023.

Rajesh, H.M., Santosh, M., 2012. Charnockites and Charnockites. *Geoscience Frontiers* 3, 737–744. https://doi.org/10.1016/j.gsf.2012.07.001.

Ramakrishnan, M., Viswanatha, M.N., Swami Nath, J., 1976. Basement-cover relationships of Peninsular Gneisses with high-grade schists and greenstone belts of southern Karnataka. *J. Geol. Soc. India* 17, 97–111 ,. https://doi.org/10.17491/jgsi/1976/170116.

Ravindra Kumar, G.R., Venkatesh Raghavan, R., 1992. The incipient charnockites in transition zone, khondalite zone and granulite zone of South India: controlling factors and contrasting mechanisms. *J. Geol. Soc. India* 39(4), 293–302. https://doi.org/10.17491/jgsi/1992/390403.

Rekha, S., Bhattacharya, A., Chatterjee, N., 2014. Tectonic restoration of the Precambrian crystalline rocks along the west coast of India: Correlation with eastern Madagascar in East Gondwana. *Precamb. Res* 252, 191–208,. https://doi.org/10.1016/j.precamres.2014.07.013.

Rekha, S., Viswanath, T.A., Bhattacharya, A., Prabhakar, N., 2013. Meso/Neoarchean crustal domains along the north Konkan coast, western India: The Western Dharwar Craton and the Antongil Masora Block (NE Madagascar) connection. *Precamb. Res* 233, 316–336. https://doi.org/10.1016/j.precamres.2013.05.008.

Rogers, J.J.W., 1986. The Dharwar Craton and the assembly of Peninsular India. *J. Geol* 94, 129–143. https://doi.org/10.1086/629019.

Santosh, M., Osanai, Y., Tsunogae, T., 2004. Ultrahigh-temperature metamorphism and deep crustal processes. *J. Mineral. Petrol. Sci* 99, 137–365. https://doi.org/10.2465/jmps.99.137.

Santosh, M., Ram Mohan, M., Tsunogae, T., Shaji, E., Satyanarayanan, M., 2014. Cryogenian alkaline magmatism in the Southern Granulite Terrane, India: Petrology, geochemistry, zircon U–Pb ages and Lu–Hf isotopes. *Lithos* 208-209, 430–445,. https://doi.org/10.1016/j.lithos.2014.09.016.

Santosh, M., Tsunogae, T., 2003. Extremely high-density pure CO_2 fluid inclusions in a garnet granulite from southern India. *J. Geol* 111, 1–16,. https://doi.org/10.1086/344578.

Santosh, M., Yang, Q.Y., Shaji, E., Ram Mohan, M., Tsunogae, T., Satyanarayanan, M., 2016. Oldest rocks from Peninsular India: Evidence for Hadean to Neoarchean crustal evolution. *Gondwana Res* 29, 105–135,. https://doi.org/10.1016/j.gr.2014.11.003.

Santosh, M., Yang, Q.Y., Shaji, E., Tsunogae, T., Ram Mohan, M., Satyanarayanan, M., 2015. An exotic Mesoarchean microcontinent: the Coorg Block, southern India. *Gondwana Res* 27, 165–195,. https://doi.org/10.1016/j.gr.2013.10.005.

Sarma, D.S., Fletcher, I.R., Rasmussen, B., McNaughton, N.J., Ram Mohan, M., Groves, D.I., 2011. Archaean gold mineralization synchronous with late cratonization of the Western Dharwar Craton India: 2.52 Ga U–Pb ages of hydrothermal monazite and xenotime in gold deposits. *Mineralium Deposita* 46, 273–288,. https://doi.org/10.1007/s00126-010-0326-3.

Shand, S.J., 1943. *The Eruptive Rocks*. 2nd edn ed., John Wiley & Sons, New York.

Srikantappa, C., Raith, M., Tourtet, J.L.R., 1992. Synmetamorphic high density carbonic fluids in the lower crust: evidence from the Nilgiri Granulites, S. India. *J. Petrol* 28, 803–834,. https://doi.org/10.1093/petrology/33.4.733.

Streckeisen, A., 1974. Classification and nomenclature of plutonic rocks. *Geologische Rundschau* 63, 773–786,. https://doi.org/10.1007/BF01820841.

Stähle, H.J., Raith, M., Hoernes, S., Delfs, A., 1987. Element mobility during incipient granuliteformation in Kabbaldurga, southern India. *J. Petrology* 28, 803–834. https://doi.org/10.1093/petrology/28.5.803.

Sunil, P.S., Radhakrishna, M., Kurian, P.J., Murty, B.V.S., Subrahmanyam, C., Nambiar, C.G., Arts, K.P., Arun, S.K., Mohan, S.K., 2010. Crustal structure of the western part of the Southern Granulite Terrain of Indian Peninsular Shield derived from gravity data. *J. Asian Earth Sci* 39, 551–564,. https://doi.org/10.1016/j.jseaes.2010.04.028.

Swami Nath, J., Ramakrishnan, M., 1981. Early Precambrian supracrustal sequences of southern Karnataka. *Geol. Surv. India Memoir* 112, 350.

Swami Nath, J., Ramakrishnan, M., Viswanatha, M.N., 1976. Dharwar stratigraphic model and Karnataka craton evolution. *Rec. Geol. Surv. India* 107, 149–175.

Taylor, P.N., Chadwick, B., Moorbath, S., Ramakrishnan, M., Viswanatha, M.N., 1984. Petrography, chemistry and isotopic ages of Peninsular gneiss, Dharwar acid volcanic rocks and the Chitradurga granite with special reference to the late Archaean evolution of the Karnataka Craton. *Precambrian Res* 23, 349–375,. https://doi.org/10.1016/0301-9268(84)90050-0.

Tomson, J.K., Bhaskar Rao, Y.J., Vijaya Kumar, T., Mallikarjuna Rao, J., 2006. Charnockite genesis across the Archean–Proterozoic terrane boundary in the South Indian Granulite Terrane: Constraints from major-trace element geochemistry and Sr-Nd isotopic systematics. *Gondwana Research* 10, 115–127,. https://doi.org/https://doi.org/10.1016/j.gr.2005.11.023.

Trendall, A.F., Laeter, J.R., Nelson, D.R., Mukhopadhyay, D., 1997. A precise zircon U–Pb age for the base of the BIF of the Mulaingiri Formation (Bababudan Group, Dharwar Supergroup) of the Karnataka Craton. *J. Geol. Soc. India* 50, 161–170,. https://doi.org/10.17491/jgsi/1997/500204.

Yang, Cheng.Xue, Santosh, M., Lloyd, J.C., Glorie, S., Gao, P., Yu, B., Anilkumar, Y., Anoop, K.S., Kim, Sung.Won, 2023. The Coorg Block, southern India: Insights from felsic and mafic magmatic suites on Mesoarchean plate tectonics and correlation with supercontinent Ur. *Gondwana Res* 118, 1–36,. https://doi.org/10.1016/j.gr.2023.02.015.

Yu, B., Santosh, M., Wang, M..X., Yang, C..X., 2022. Paleoproterozoic emplacement and Cambrian ultrahigh temperature metamorphism of a layered magmatic intrusion from the Central Madurai Block, southern India: From Columbia to Gondwana. *Geosci. Front* 13, 101260, 1–16,. https://doi.org/10.1016/j.gsf.2021.101260.

